

# Excitonic and Charge Transfer States in Oligomeric 9,10-Anthrylene Chains

Ralf Fritz and Wolfgang Rettig<sup>\*,†,‡</sup>

Iwan-N.-Stranski Institut, Technische Universität Berlin, Str. des 17. Juni 112, D-10623 Berlin, FRG, and  
W. Nernst-Inst. f. Phys. & Theor. Chemie, Humboldt-Univ. Berlin, Bunsenstr. 1, D-10117 Berlin, FRG

Katsura Nishiyama and Tadashi Okada<sup>\*</sup>

Department of Chemistry, Faculty of Engineering Science, and Research Center for Extreme Materials,  
Osaka University, Toyonaka, Osaka 560, Japan

Uwe Müller and Klaus Müllen

Max-Planck-Institut für Polymerforschung, Ackermannweg 10, D-55128 Mainz, FRG

Received: December 4, 1996<sup>⊗</sup>

The dimer (9,9'-bianthryl), trimer, and tetramer of anthracene, linked in the 9,10-position and equipped with solubility-increasing alkyl substituents, were investigated by steady state and time-resolved fluorescence spectroscopy and by transient absorption. In polar solvents, charge separation occurs with dipole moments increasing with chain length. The ease of charge separation depends on the energetic competition of the charge transfer (CT) and the lowest excitonic state. It is especially favorable for the tetramer in which the CT state was observed even in a 77 K frozen alcoholic matrix.

## 1. Introduction

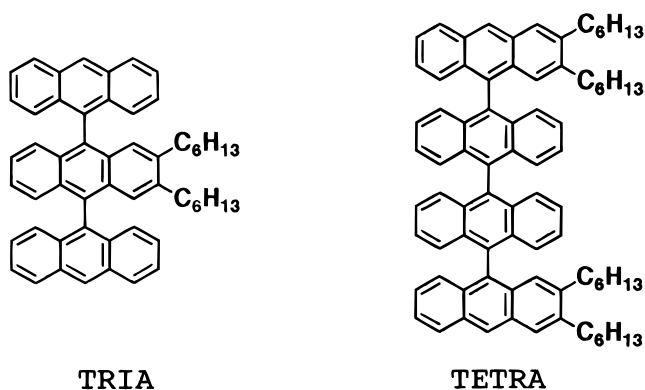
The solvent-induced excited state charge separation in 9,9'-bianthryl (BA) has been the subject of numerous studies both in solution<sup>1–22</sup> and in the gas phase (supersonic jets).<sup>23–27</sup> BA shows dual fluorescence in polar solvents,<sup>1</sup> with a structured short wavelength band (B band or LE (locally excited), in fact the excitonic band, see below) and a charge transfer (CT or A) band. The CT band has been explained within the context of twisted intramolecular charge transfer (TICT) states,<sup>5,7,14–17,28,29</sup> and this theory has been successfully used to predict new biaryls with CT properties.<sup>7,30</sup> Although the charge transfer nature of the emissive state of BA in polar solvents has been proven by the similarity of the transient absorption spectra to those of the radical anion and cation and by the comparison of absorption and emission kinetics,<sup>11–13</sup> there still seems to exist some controversy about the nature of this state. Varma et al. attributed the emission in dioxane to a solute–solvent exciplex, with no reference to an intramolecular charge separation.<sup>22</sup> Wortmann et al. determined the intramolecular twist potential in the LE state from the temperature dependence of the fluorescence spectra in alkane solution and found a strongly increased rotational barrier as compared to the potential deduced from supersonic jet studies.<sup>19</sup> The rotational barriers for slightly polar solvents increase even further if a one-state model comprising only the LE state is used.<sup>20</sup> The questions can therefore be asked whether the CT component is responsible for the result of increased barriers in solution and whether a minor CT contribution might already be present in alkane solvents. Such a minor CT contribution even in nonpolar solvents would also be consistent with excited state dipole moment determinations of BA with the electric field method<sup>18</sup> and with transient dielectric loss measurements.<sup>21</sup>

In this contribution, we compare BA to longer chain anthracene oligomers and study the spectral and photophysical

properties. It will be shown that trimer and tetramer also exhibit photoinduced charge separation and that the solvatochromic slope of the tetramer in the high-polarity region is significantly larger than that for bianthryl in spite of the approximately doubled molecular volume. This is consistent with a considerably increased dipole moment for the tetramer, indicating a larger charge separation distance for compounds with an increased number of anthracene chromophores. CT state formation is most prominent for the longest member of the series.

## 2. Experimental Section

**2.1. Synthesis.** 2',3'-Dihexyltri-9,10-anthrylene (1) (TRIA) has been synthesized by reaction of 9-lithioanthracene with anthraquinone, followed by reductive aromatization of the intermediate dihydroxy species with HI/H<sub>3</sub>PO<sub>2</sub> and chromatography on silica gel (60% yield). 2,2''',3,3''''-Tetrahexyltetra-9,10-anthrylene (2) (TETRA) is formed by treatment of 10,10'



bianthronylidene with 9-lithioanthracene in a reaction sequence analogous to the trimer synthesis (31% yield).<sup>31–33</sup> To sustain sufficient solubility of the novel oligo(9,10-anthrylene)s in common organic solvents, solubilizing alkyl substituents were introduced at the 2- and 3-positions of the anthracene rings

<sup>†</sup> Technische Universität Berlin.

<sup>‡</sup> Humboldt-Univ. Berlin.

<sup>⊗</sup> Abstract published in *Advance ACS Abstracts*, March 15, 1997.

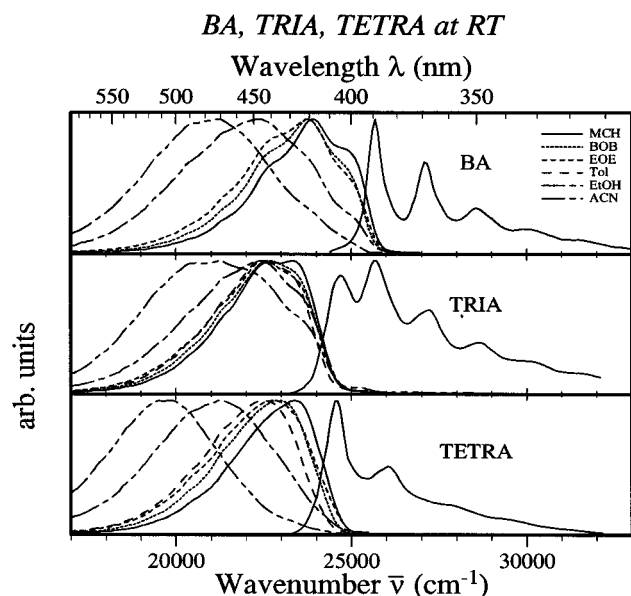


**Figure 1.** Comparison of absorption and fluorescence spectra of BA, TRIA, and TETRA in solvents of different polarity at room temperature: methylcyclohexane (MCH), di-*n*-butyl ether (BOB), diethyl ether (EOE), toluene (Tol), ethanol (EtOH), and acetonitrile (ACN).

during the first step of the reaction sequence.<sup>34,35</sup> Further purification of **1** and **2** was achieved by repeated column chromatography on silica gel, recrystallization from methylene chloride/hexane (1:1), and size exclusion chromatography. 2,6-Di-*tert*-butylantracene (**3**) and 2,3-dihexylantracene (**4**) were prepared according to procedures previously described.<sup>36,37</sup> Compounds **3** and **4** were purified by column chromatography and repeated recrystallization from hexane. The structure proof of compounds **1**, **2**, **3**, and **4** rests on IR, NMR, and mass spectroscopy. The purity of all samples was verified by thin layer chromatography and/or HPLC.

**2.2. Spectroscopy.** Time-resolved absorption spectra have been measured by means of femtosecond pulse and picosecond laser systems. The output pulse of a dye laser (pyridine 1) synchronously pumped with the second harmonics of a CW mode locked Nd:YAG laser was amplified with a three-stage dye cell pumped by a 10 Hz Q-switched YAG laser. The fundamental light pulse of the dye amplifier (Spectra Physics, 710 nm, 300 fs, 0.3 mJ) was frequency doubled and used for the excitation of the sample. The remaining fundamental light was focused into D<sub>2</sub>O, producing a white light continuum which was used as a probe light to detect the transient absorption in the subpicosecond time region.<sup>38</sup> A 10 ps dye laser system (Quantel Picochrome) was used for the measurements from ca. 10 ps up to the nanosecond time region.<sup>39</sup> All samples were deaerated by flushing a nitrogen gas stream before the measurements. Spectrograde solvents were used without further purification.

Fluorescence lifetimes for aerated solutions were determined with the single-photon counting method using synchrotron radiation from BESSY (Berlin) as the excitation light source and the equipment described elsewhere.<sup>40</sup> Corrected fluorescence spectra were measured using either Perkin-Elmer 650–60 or Hitachi 850E spectrophotofluorometers.

### 3. Results

#### 3.1. Steady State Spectra and Fluorescence Lifetimes.

The steady state absorption and fluorescence spectra of BA, TRIA, and TETRA in solvents of different polarity are displayed in Figure 1. A clear red shift of the emission is observed for

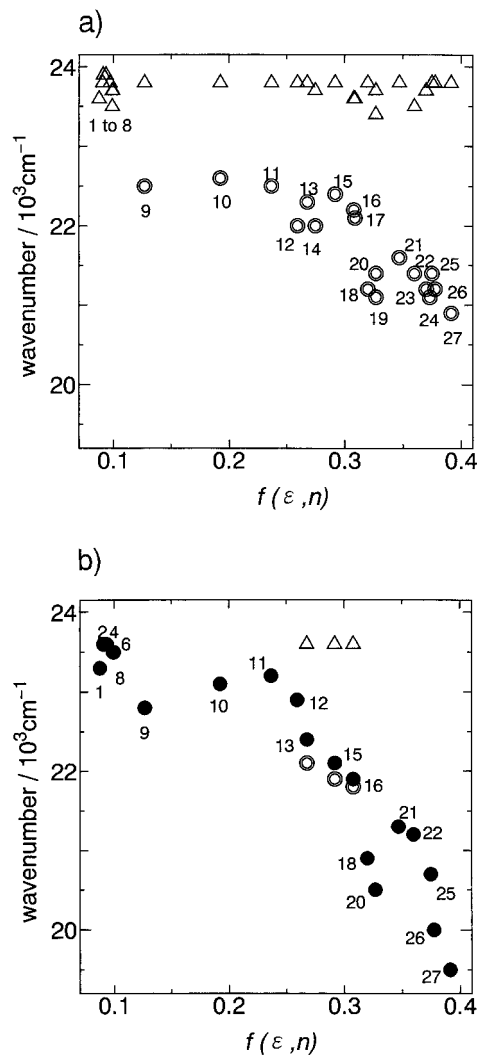


**Figure 2.** Fluorescence solvatochromic plot for (a) TRIA (CT maxima from decomposed spectra) and (b) TETRA (points labeled with open circles correspond to decomposed CT component, filled circles for undecomposed spectra; triangles indicate the LE band). The solvents are indicated as follows: 1, tetrachloroethylene; 2–8, alkanes; 9, toluene; 10, dibutyl ether; 11, 12, diethyl ether; 13–15, ethyl acetate; 16, tetrahydrofuran; 17, 18, dichloromethane; 19–23, butyronitrile; 24, DMSO; 25, acetone; 26, DMF; 27, acetonitrile.

the strongly polar solvents ethanol and acetonitrile, whereas the absorption spectra exhibit only marginal changes. In all cases, a short wavelength shoulder remains in the emission spectrum at approximately the 0–0 band of the emission in alkanes, indicative of the multiple nature of the emission, CT, and LE bands. For a given solvent, e.g. acetonitrile, the LE contribution is strongest in TRIA, intermediate in BA, and weakest in TETRA.

Figure 2 shows solvatochromic plots for TRIA and TETRA, derived from the decomposition of the spectra into CT and LE components by subtracting the suitably shifted and weighted alkane spectrum from the total spectrum, similar to the method used in the literature.<sup>5</sup> There is an alternative approach to subtract a Gaussian-shaped CT band from the total spectrum.<sup>6</sup> The results of that decomposition lead to a considerably smaller weight of the CT band. As it is not yet clear which is the correct way of spectral decomposition, we prefer to use the first method. For TETRA, due to the reduced structural features of the spectra (see Figure 1), decomposition for more polar solvents ( $\epsilon > 10$ ) proved to be unnecessary, so the maximum of the undecomposed spectra are shown, together with some decomposed points. Decomposition hardly affects the results for the fluorescence

**TABLE 1: Solvatochromic Slope,  $m$ , Determined from the High-Polarity Portion of the Solvatochromic Plots of Fluorescence Band Maxima in Figure 2a,b and Estimated Dipole Moment in the CT State,  $\mu_{es}$ , by Using the Different Onsager Radii  $a_o$**

	BA	TRIA	TETRA
$m, 10^3 \text{ cm}^{-1}$	-14	-14	-26
$a, \text{Å}^a$	6	8	10
$\mu, \text{Debye}$	20	29	53
$a, \text{Å}^b$	6	9	12
$\mu, \text{Debye}$	20	35	70
$a, \text{Å}^c$	6	7.5	8.6
$\mu, \text{Debye}$	20	27	42
$\mu, \text{Debye}^d$	21	42	63

<sup>a</sup> Sphere radius which covers the anthrylene part without considering hexyl units. <sup>b</sup> Sphere radius which covers the whole molecule including hexyl units. <sup>c</sup> Estimated from the molecular weight according to the equation where  $a(i) = (M_w(i)/M_w(\text{BA}))^{1/3} a(\text{BA})$ ;  $i = \text{TRIA, TETRA}$ ;  $M_w = \text{molecular weight}$ ; and  $a = 6 \text{ Å}$  is assumed. <sup>d</sup> Dipole moment calculated from the point charge pair located on the center of the anthryl units of both ends. Assumed bond lengths are 1.4 Å for aromatic C-C bonds and 1.54 Å for the bonds between anthryl units.

**TABLE 2: Fluorescence Decay Times,  $\tau_f$  (in ns), and Quantum Yields of the Total Fluorescence,  $\phi_f^{(A+B)}$ , As Determined at Room Temperature in Nondegassed Solutions, and the Effective Radiative Rate Constant ( $k_f = \phi_f^{(A+B)}/\tau_f$  (in  $10^7 \text{ s}^{-1}$ )**

	A	BA	TRIA	TETRA
$\tau_f$ (alkanes) <sup>a</sup>	3.3, 5.0 <sup>e</sup>	4.1	5.0	4.1 <sup>b</sup>
$\tau_f$ (ethanol)	3.7, 5.5 <sup>e</sup>	12.9 <sup>c</sup>	11	13 <sup>d</sup>
			23 <sup>f</sup>	22 <sup>f,g</sup>
$\phi_f^{(A+B)}$ (alkanes) <sup>a</sup>	0.33 <sup>e</sup>	0.42	0.6	0.81
$\phi_f^{(A+B)}$ (ethanol)	0.30 <sup>e</sup>	0.25	0.42	0.31
$\langle k_f \rangle$ (alkanes) <sup>a</sup>	6.4 <sup>e</sup>	10.2	12	20
$\langle k_f \rangle$ (ethanol)	5.2 <sup>e</sup>	1.9	3.8	2.4

<sup>a</sup> In methylcyclohexane or hexane measured at 430 or 450 nm. <sup>b</sup> In degassed methylcyclohexane-isopentane mixture. <sup>c</sup> At 485 nm. <sup>d</sup> At 500 nm. <sup>e</sup> For degassed solutions from ref 46. <sup>f</sup> In degassed acetonitrile. <sup>g</sup> Nonexponential, long component is given.

**TABLE 3: Solvent Dependence of the Ratio of Fluorescence Quantum Yields of A and B Bands,  $\phi_f^A/\phi_f^B$ , for Degassed Solutions As Determined by Band Decomposition**

	butyl acetate	ethyl acetate	THF	butyronitrile	DMF
TRIA	0.7	1.0	1.1	1.4	2.0
TETRA	4.7	6.4	13		

maximum for TETRA even in medium polar solvents, whereas for TRIA, due to its strongly increased LE contribution, the decomposition is very important to extract the correct wavelengths of the CT band. For instance, the estimated ratio of the fluorescence quantum yield  $\Phi_{LE}/\Phi_{CT}$  is 0.15 for TETRA but 0.88 for TRIA in ethyl acetate. In the high-polarity end of the solvatochromic plots (Figure 2a,b), where the data are least affected by the contribution of LE emission, the solvatochromic slopes are clearly different and strongest for TETRA (Table 1).

Tables 2 and 3 summarize the relevant photophysical data for the systems at room temperature. Whereas the fluorescence decay times,  $\tau_f$ , are little affected by solvent polarity for anthracene, they lengthen dramatically for the polyaryl systems in polar solvents, indicating that the emissive state is different in the two types of solvent. The effective fluorescence rate constants  $\langle k_f \rangle$  as calculated from  $\Phi_{f(A+B)}/\tau_f$  exhibit a strong decrease in the more polar solvents, consistent with the previous results for BA<sup>4</sup> and with the forbidden nature of the A-emission.<sup>4,28-30</sup> Table 3 demonstrates how the relative weight of the A-emission increases with solvent polarity from TRIA to TETRA.

The fluorescence and fluorescence excitation spectra of the

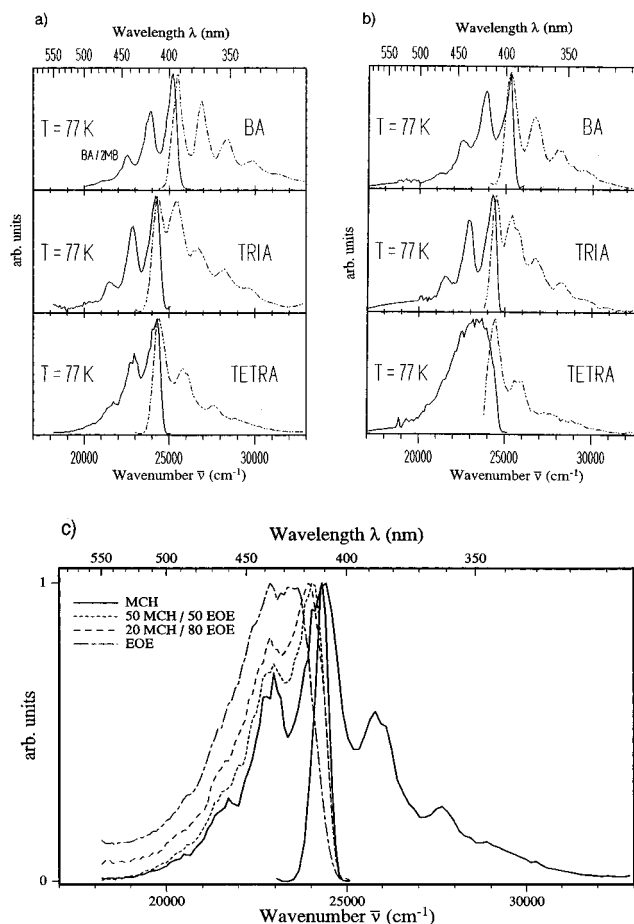


**Figure 3.** Fluorescence excitation and emission spectra of BA, TRIA, and TETRA at 77 K in (a) methylcyclohexane (2-methylbutane for BA) and (b) ethanol glass. In (c), the effect on the fluorescence spectrum of TETRA by adding various proportions of diethyl ether to methylcyclohexane is shown.

**TABLE 4: Fluorescence Decay Times (in ns) of Various Anthracenes and Anthracene Oligomers at 77 K**

solvent	BA	TRIA	TETRA	A <sup>a</sup>	DHA <sup>b</sup>	DTBA <sup>c</sup>	TB9A <sup>d</sup>
alkane <sup>e</sup>	10.3	5.5	4.1	5.1 <sup>f</sup> (12)	15 <sup>f</sup> (5.3)	12.5	
ethanol	6.8 <sup>f</sup>	7 <sup>f</sup>	18 <sup>f</sup>	5 <sup>g</sup>	21 <sup>f</sup>	14.9	15.4
	(15)	(17)	(5)		(8.2)		

<sup>a</sup> Anthracene. <sup>b</sup> 2,3-Dihexylanthracene. <sup>c</sup> 2,6-Di-*tert*-butylanthracene. <sup>d</sup> 9-*tert*-Butylanthracene. <sup>e</sup> 3-Methylpentane or methylcyclohexane/isopentane mixture. <sup>f</sup> Main decay component, minor one given in parentheses. <sup>g</sup> Nonexponential.

compounds are compared in Figure 3 for frozen solvent matrices at 77 K. In alkanes (Figure 3a), the fluorescence is a good mirror image of the absorption. For ethanol glass (Figure 3b), TRIA and BA behave similar to alkane glasses, but TETRA shows a broadened emission band which can be interpreted as indicating a contribution of CT emission. This is supported by the measurements in mixtures of methylcyclohexane with diethyl ether (Figure 3c) which indicate an increased contribution of the unstructured spectral component with increasing ether content. This experiment also rules out the possibility of these effects being due to specific interactions with the protic solvent. Table 4 summarizes decay data for the oligoanthracenes and various model anthracene monomers at 77 K. Anthracene and 2,3-dihexylanthracene exhibit a complicated decay behavior dominated by short lifetimes in the former and long lifetimes in the latter case. For 2,6-di-*tert*-butylanthracene and 9-*tert*-butylanthracene (TB9A), however, only the long lifetime component around 15 ns remains. The long lifetime component

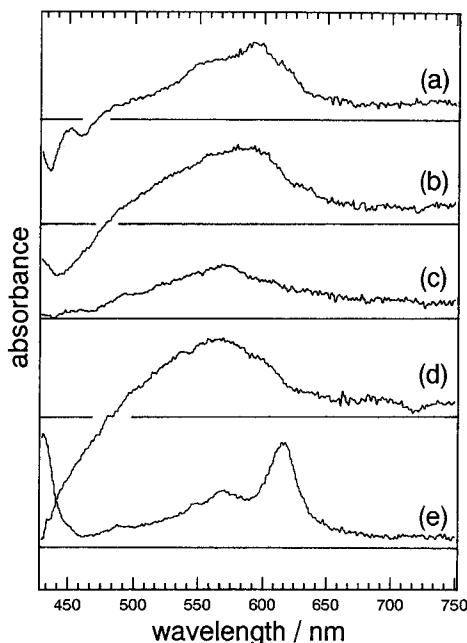


**Figure 4.**  $S_n \leftarrow S_1$  absorption spectra of TRIA, TETRA, and DHA detected at 100 ps after the laser excitation in the methylcyclohexane/isopentane mixed solvent. (a) TRIA at 77 K, (b) TRIA at 293 K, (c) TETRA at 77 K, (d) TETRA at 293 K, and (e) DHA at 293 K.

may be an indication of cluster formation at low temperature, especially for the anthracenes with long alkane chains. The shortening of the lifetime for the higher anthracene oligomers is indicative of a more allowed radiative transition in accordance with the exciton model.<sup>30,41</sup> In ethanol, the decay behavior of the oligomers is more complicated than in alkanes. Especially for TETRA, a considerable weight of a long lived component is observed which can be identified with the CT component observed in the spectra (Figure 3c).

**3.2. Transient Absorption Spectra.** The  $S_n \leftarrow S_1$  absorption spectra of TRIA and TETRA observed at 100 ps after the laser excitation in a nonpolar solvent, methylcyclohexane/isopentane (1:1 in volume), at 293 and 77 K are illustrated in Figure 4. Negative absorbances observed in the short wavelength region at 420–460 nm are due to the induced fluorescence which corresponds to the LE fluorescence of the perpendicular conformation at 77 K and the twisted one at 293 K. For TRIA, the spectral shape of the  $S_n \leftarrow S_1$  absorption measured at 77 K (Figure 4a) is similar to that of anthracene or 2,3-dihexylanthracene (DHA, Figure 4e) but somewhat broadened and blue-shifted, whereas at 293 K (Figure 4b) it becomes less structured than anthracene or DHA. These behaviors seem to be general in anthrylenes examined here and are also observed in the case of BA.<sup>11</sup> This indicates that the two anthracene chromophores are perpendicular to each other at 77 K, corresponding to the conformation in the ground state. The broadening of the spectra at 293 K indicates an intramolecular rotational relaxation from the perpendicular Frank–Condon (FC) state to an inclined structure (relaxed state). On the other hand, TETRA exhibits somewhat broadened absorption spectra even at 77 K (Figure 4c,d), and the whole absorption band seems to be blue-shifted compared to TRIA and BA.

Time-resolved transient absorption spectra of TETRA in cyclohexane are shown in Figure 5. The structured spectrum obtained at 1 or 4 ps after the excitation is rather similar to that observed at 77 K, which is attributed to a large contribution from the perpendicular conformation between the anthracene chromophores. The spectrum gradually changes its shape with time while getting broader, and the absorption maximum shifts

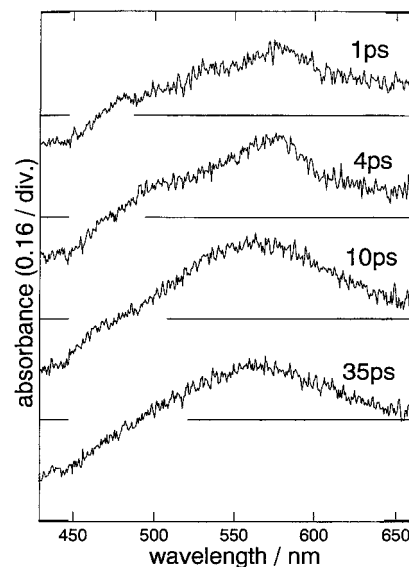


**Figure 5.** Time-resolved absorption spectra of TETRA in cyclohexane. Detecting times after the excitation pulse are given in the figure.

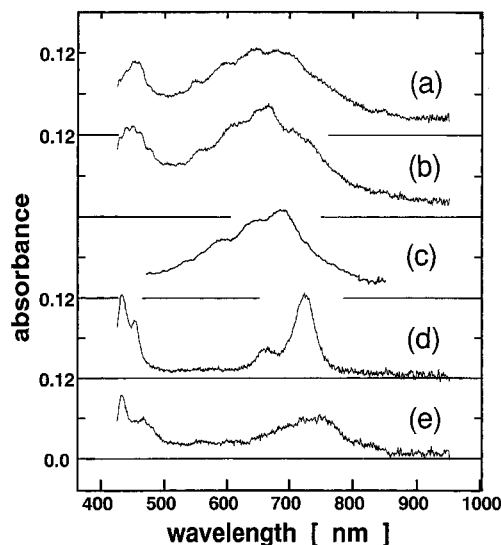


**Figure 6.** Absorption spectra of the excited state of (a) TRIA in acetonitrile, (b) TETRA in DMF, and (c) BA in acetonitrile. Absorption spectra of (d) DHA cation and (e) DHA anion in acetonitrile obtained by addition of DCNB and DMA in solution, respectively.

toward the blue, which corresponds to the formation of the relaxed state within the time of 30 ps after excitation. Such spectral changes were also observed for TRIA. By analyzing the transient absorption spectra, we can obtain the relaxation time,  $\tau$ , for the geometrical change to the relaxed state. Obtained relaxation times are  $\tau \cong 11$  ps for TRIA and 15 ps for TETRA, in close agreement with the value of BA,  $\tau \cong 10$  ps.<sup>11</sup>

In polar solvents, transient absorption spectra corresponding mainly to the CT state are observed for TRIA and TETRA (Figure 6). The spectra are given at 100 ps, but there are no remarkable changes in the absorption band shapes up to several nanoseconds. All spectra including BA are broad, with absorption maxima at 650–680 nm, and different in the details of the observed structure. The absorption spectra of DHA cation and anion radicals obtained by adding *p*-dicyanobenzene (DCNB) and *N,N*-dimethylaniline (DMA) in acetonitrile solution, respectively, are also shown in Figure 6d,e. The bands in the 400–500 nm region observed in Figure 6d,e are mainly due to the DHA triplet (425 nm), DCNB anion (d), and DMA cation (e). We should emphasize here that the observed spectrum of

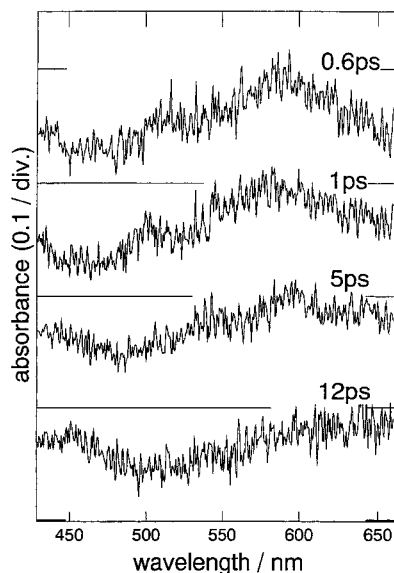


**Figure 7.** Time-resolved absorption spectra of TRIA in DMF at 293 K.

TRIA in the polar solvent acetonitrile could not be exactly reconstructed by the superposition of the unshifted absorption spectra of the radical cation and anion of anthracene, 9-methylanthracene and/or DHA, as in the case of BA.<sup>11</sup> For TETRA, however, the spectra are reproduced by the sum of the absorption bands of the 9-methylanthracene cation and DHA anion. Thus in the case of TETRA, taking into consideration the large solvatochromic shifts and slope at highly polar solvents, there may be the possibility to produce a long distance separated ion pair state with a large dipole moment which is not observed in the case of BA or TRIA.

Femtosecond time-resolved measurements were also performed in polar solvents. For TRIA in DMF (Figure 7), the spectral origin of the broad band with maximum at ca. 590 nm, as detected at 0.6 ps after the excitation, may be assigned to the  $S_n \leftarrow S_1$  absorption spectrum which was observed in the 77 K glass matrix solvent (Figure 4a). The characteristic absorption band with the maximum at 590 nm which should be ascribed to the perpendicular FC state is decreasing with time, while the CT absorption band is becoming dominant, in particular in the wavelength region longer than 600 nm. Similar trends were also observed for TETRA in DMF. The rise time of the CT state,  $\tau_{CT}$ , was obtained by analyzing the absorbance changes at longer wavelengths near 630 nm. Both  $\tau_{CT}$  for TRIA and for TETRA in DMF are within the time range of 1.1–1.5 ps. The values of  $\tau_{CT}$  for TRIA and TETRA are rather similar to the value for BA in acetonitrile,  $\tau_{CT} \cong 1.8$  ps, although the solvent used here is a different one.<sup>11</sup>

## 4. Discussion

**4.1. The Excitonic State.** In alkanes,  $k_f$  increases from A to BA to TETRA (Tables 2 and 4), consistent with the exciton model for a linear array of chromophores<sup>41</sup> where the lowest excitonic state carries the transition moment of several monomers. Thus, for TETRA, the emission becomes highly allowed, and very large fluorescence quantum yields are reached (Table 2).

The observation of biexponential decays for the different anthracene derivatives in solution at 77 K (Table 4) may seem puzzling at first. It can, however, be explained by the possible formation of ground state dimers or higher clusters. These are expected to possess a larger transition moment due to excitonic interaction, and thus a shorter lifetime should result. We

therefore assign the short lifetime component to dimers/clusters. This assignment is supported by the fact that the short component is much larger for anthracene than for DHA and is missing for DTBA in alkane solvents, consistent with the expected steric hindrance of larger alkyl groups to a sandwich-type dimer.

**4.2. Dipole Moments.** The dipole moment  $\mu_e$  of the excited CT state can be estimated by means of the Lippert–Mataga–Liptay theory,<sup>42–44</sup> neglecting the ground state dipole moment and the solute polarizability (eq 1).

$$hc\tilde{\nu}_{\max} = hc\tilde{\nu}_{\max}(0) - (2\mu_e^2/a_o^3)[f(\epsilon, \tilde{\nu})] \quad (1)$$

$$f(\epsilon, \tilde{\nu}) = [(\epsilon - 1)/(2\epsilon + 1)] - 1/2[(n^2 - 1)/(2n^2 + 1)]$$

where  $\tilde{\nu}_{\max}(0)$  is the gas phase fluorescence maximum (in  $\text{cm}^{-1}$ ),  $n$  the solvent refractive index,  $\epsilon$  the solvent dielectric constant, and  $a_o$  the Onsager radius of the solvent cavity.

There are different approaches possible for comparing the solvatochromic behavior of molecules of different size and shape. In view of these uncertainties we will consider the extreme possibilities only: (i)  $a_o$  increases linearly with the long axis of the molecule.<sup>1</sup> (ii)  $a_o$  increases more weakly, proportional to the third root of the molecular volume. A convenient approach to  $a_o$  in this case is from molecular weight and density.

Table 1 summarizes the results for the dipole moments obtained using these two approximations and also contains the comparison to the dipole moment values calculated from a point charge model with the charge residing on the most distant anthracene rings (iii).

The results indicate that the dipole moment increases considerably with the number of anthracene units. This qualitative result is independent of the details of the evaluation procedure and of the refinement of the Onsager model used.

Information on the electronic nature of the CT state can also be gained from the photophysical parameters. The  $k_f$  and  $\tau_f$  values in alkane as compared to polar solvents are additional evidence that the nature of the emissive state changes.

In ethanol, the  $k_f$  values are considerably lower than in alkanes and point to the involvement of a radiatively forbidden state, consistent with the TICT model.<sup>28,29</sup> It should, however, be mentioned that depending on the extent of vibronic interaction and the width of the rotational distribution function in the TICT state, TICT emission can also become allowed.<sup>45,46</sup> This has recently been described for the related case of 5,5'-biperylenyl,<sup>30</sup> a somewhat less symmetric molecule than BA and the other anthracene oligomers.

If the short lifetime components are attributed to parasitic processes (e.g. intersystem crossing (isc) to a nearby triplet state and equilibration), the absence for the *tert*-butylanthracene derivatives seems to indicate a simpler photophysical behavior than that for anthracene itself. This is probably linked with the energetically lower  $S_1$  state of the substituted anthracenes. The linking of anthracene units in the oligomers still further lowers the singlet states (see Figure 1) such that it is reasonable to assume that isc does not play an important role in the anthracene oligomers and in TB9A or DTBA. We can thus take the observed lifetime as a good measure for the inverse of the fluorescence rate constant  $k_f^{\text{LE}}$  of the LE or excitonic state.

**4.3. Availability of the CT State.** The transient absorption measurements in conjunction with the solvatochromic fluorescence red shifts are clear evidence for photoinduced charge separation. This follows, on the one hand, from the resemblance of the transient spectra in polar solvents to the sum of the anthracene anion and cation spectra as already described for

bianthryl<sup>11,13,30</sup> and, on the other hand, from the nonzero excited state dipole moment deduced from fluorescence solvatochromism. Similar to BA, the ground state dipole moment for the compounds investigated is close to zero, and charge separation involves a symmetry-breaking process.<sup>4,5,11,16,17</sup> For TRIA and TETRA, several charge-separated states are possible, involving different pairs of anthracene donors/acceptors, which may be separated by zero, one, or two uncharged anthracene rings and possess correspondingly increasing dipole moments due to the large charge separation distance. It is not very clear at the present stage of our investigation whether the large charge separation distance is actually realized in the case of TETRA in polar solvents at room temperature. The observed experimental results may be explained for both cases, (a) charge separation between adjacent anthracene rings and (b) ion pair separated by uncharged anthracene rings, as described below. (a) The rise times of the charge transfer state obtained by the transient absorption measurements for TRIA and TETRA in DMF are rather close to that of BA. The rate of the charge shift reaction in TRIA and TETRA should be slower than that of the initial charge separation reaction since the free energy change in the charge shift reaction is much smaller than that of the charge separation, which indicates the possibility that the adjacent anthracene rings are involved in the charge separation in the case of TETRA and the larger dipole moments obtained from the solvatochromic plots might be ascribed to an overestimation of the Onsager radii. (b) The solvatochromic slope of TETRA is about two times larger compared to those of BA and TRIA, which are the same slopes as indicated in Table 1. Furthermore, the transient absorption spectra of TETRA in polar solvent can be reproduced by the sum of the absorption bands of 9-methylanthracene cation and DHA anion as described in section 3.2. The large anthrylene chains may prevent the polar solvation for at least half of the charge-separated state in the case of the adjacent CT state, while the ion pair localized in the end rings has a large dipole moment stabilized by surrounding polar solvent molecules. When the charge shift reaction takes place coupled with the solvent fluctuation, rapid charge separation within some picosecond time scale would be possible. From the large dipole moment values as estimated in Table 1, there seems to be an energetic preference for the most strongly charge-separated states, but the complicated lifetime behavior observed especially for TETRA in polar solvents (Table 2) indicates the probable contribution of more than one CT state to the emission.

According to the exciton model, the excitonic interaction lowers the lowest of the excitonic states, and this can directly be observed from the red shift of the absorption spectra (Figure 1). Thus, the excitonic interaction for TETRA is larger than that for BA, but it does not seem to be larger than that for TRIA. This has direct consequences for the relative population of LE and TICT levels. The strongly increased weight of TICT emission for TETRA as compared to that for TRIA (Figure 2c, Table 3) can thus be understood by a larger energy difference between the excitonic and TICT state, i.e. by a TICT level which is lower for TETRA than for TRIA.

As judged from the spectral comparison in Figure 1, the structured spectral component for TETRA in polar solvents is even weaker than that for BA, indicating the easiest (most strongly exothermic) TICT formation for TETRA. Some of this preference for the TICT state is possibly favored by the larger size of TETRA which allows many more conformational and solvent fluctuational inhomogeneous distributions. This is evidenced for rigid frozen solvents (Figure 3) where all charge separation normally ceases for the vast majority of TICT

compounds.<sup>28,29</sup> Frozen ethanol and ether possess a dipolar inhomogeneity which causes local fields. Due to its increased size, TETRA is in contact with many more of these inhomogeneities, and symmetry breaking is more probable. From an applicational point of view, TETRA may serve as a fluorescence probe for the microscopic polarity of rigid environments, glasses, polymers, or biological matrices, probing the microheterogeneity of dielectric properties in the local surroundings.

A further applicational aspect might be developed for even longer chains of anthracene oligomers. According to the theory of Stolarczyk and Piela (SP),<sup>47</sup> the CT is energetically lowered for long oligomers of donor-acceptor chains until, eventually, it becomes close enough to the nonpolar ground state to be lowered sufficiently by electric field effects to become the ground state. This corresponds to a new macroscopic situation and opens the possibility for field-induced or photoinduced switching. SP predict three stable switchable states.<sup>47</sup> The anthracene chromophore behaves as donor and as acceptor in BA and higher oligomers, hence these compounds correspond well to the class of donor-acceptor chains described by SP.<sup>48</sup> The result of strongest TICT population, smallest LE component, and largest dipole moment for TETRA is in fact a first experimental confirmation of the theory of SP.

**Acknowledgment.** The authors thank Prof. H. Dreskamp, Braunschweig, for a gift of purified TB9A. T.O. acknowledges the support by the Grant-in-Aid for International Scientific Research Program-Joint Research (No. 05044055) from the Ministry of Education, Science, Sports, and Culture of Japan. Support by the Bundesministerium für Forschung und Technologie (project 05 414 FAB 1 and 05 5KT FAB 9) and by the Fonds der Chemischen Industrie is gratefully acknowledged.

## References and Notes

- (1) Schneider, F.; Lippert, E. *Ber. Bunsen-Ges. Phys. Chem.* **1968**, *72*, 1155. *Ibid.* **1970**, *74*, 624.
- (2) Schneider, F. Ph.D. Thesis, Technical University of Berlin, 1969.
- (3) Beens, H.; Weller, A. *Chem. Phys. Lett.* **1969**, *3*, 666.
- (4) Nakashima, A.; Murakawa, M.; Mataga, N. *Bull. Chem. Soc. Jpn.* **1976**, *49*, 854.
- (5) Rettig, W.; Zander, M. *Ber. Bunsen-Ges. Phys. Chem.* **1983**, *87*, 1143.
- (6) Müller, S.; Heinze, J. *Chem. Phys.* **1991**, *157*, 231.
- (7) Zander, M.; Rettig, W. *Chem. Phys. Lett.* **1984**, *110*, 602.
- (8) Nagarajan, V.; Brearley, A. M.; Kang, T. J.; Barbara, P. F. *J. Chem. Phys.* **1987**, *86*, 3183.
- (9) Barbara, P. F.; Kang, T. J.; Jarzaba, W.; Fonseca, T. In *Perspectives in Photosynthesis*; Jortner, J., Pullman, B., Eds.; Kluwer Academic Publishers: Dordrecht, The Netherlands, 1990; p 273. Barbara, P. F.; Jarzaba, W. *Adv. Photochem.* **1990**, *15*, 1.
- (10) Kang, T. J.; Jarzaba, W.; Barbara, P. F.; Fonseca, T. *Chem. Phys.* **1990**, *149*, 81.
- (11) Mataga, N.; Yao, H.; Okada, T.; Rettig, W. *J. Phys. Chem.* **1989**, *93*, 3383.
- (12) Okada, T.; Nishikawa, S.; Kanaji, K.; Mataga, N. In *Ultrafast Phenomena VII*; Harris, C. B., Ippen, E. P., Mourou, G. A., Zewail, A. H., Eds.; Springer Series in Chem. Phys. Vol. 53; Springer-Verlag: Berlin, 1990; p 397. Mataga, N.; Nishikawa, S.; Okada, T. *Chem. Phys. Lett.* **1996**, *257*, 327.
- (13) Lück, H.; Windsor, M. W.; Rettig, W. *J. Phys. Chem.* **1990**, *94*, 4550.
- (14) Rettig, W. In *Supramolecular Photochemistry*; Balzani, V., Ed.; NATO ASI-C Series 214; Reidel: Dordrecht, The Netherlands, 1987; p 329.
- (15) Lippert, E.; Rettig, W.; Bonacic-Koutecky, V.; Heisel, F.; Miehé, J. A. *Adv. Chem. Phys.* **1987**, *68*, 1.
- (16) Rettig, W. In *Modern Models of Bonding and Delocalization*; Liebman, J., Greenberg, A., Eds.; Molecular structure and energetics, Vol. 6; VCH: New York, 1988; Chapter 5, p 229.
- (17) Rettig, W. *Proc. Indian Acad. Sci., Chem. Sci.* **1992**, *104*, 89.
- (18) Baumann, W.; Spohr, E.; Bischof, H.; Liptay, W. *J. Lumin.* **1987**, *37*, 227.
- (19) Wortmann, R.; Elich, K.; Lebus, S.; Liptay, W. *J. Chem. Phys.* **1991**, *95*, 6371.

- (20) Wortmann, R.; Lebus, S.; Elich, K.; Assar, S.; Detzer, N.; Liptay, W. *Chem. Phys. Lett.* **1992**, *198*, 220.
- (21) Toubanc, T. B.; Fessenden, R. W.; Hitachi, A. *J. Phys. Chem.* **1989**, *93*, 2893.
- (22) Visser, R. J.; Weissenborn, P. C. M.; van Kan, P. J. M.; Varma, C. A. G. O.; Warman, J. M.; de Haas, M. *J. Chem. Soc., Faraday Trans 2* **1985**, *81*, 689. Müller, S.; Heinze, J. *Chem. Phys.* **1991**, *157*, 231.
- (23) Yamasaki, K.; Arita, K.; Kajimoto, O. *Chem. Phys. Lett.* **1986**, *123*, 277.
- (24) Kajimoto, O.; Yamasaki, K.; Arita, K.; Hara, K. *Chem. Phys. Lett.* **1986**, *125*, 184.
- (25) Honma, K.; Kajimoto, O. *J. Chem. Phys.* **1994**, *101*, 1752. Kajimoto, O. In *Dynamics of Excited Molecules*; ed. K. Kuchitsu, K., Ed.; Elsevier: Amsterdam, 1994; p 382.
- (26) Khundkar, L. R.; Zewail, A. H. *J. Chem. Phys.* **1996**, *84*, 1302.
- (27) Subaric-Leitis, A.; Monte, C.; Roggan, A.; Rettig, W.; Zimmermann, P.; Heinze, J. *J. Chem. Phys.* **1990**, *93*, 4543.
- (28) Grabowski, Z. R.; Rotkiewicz, K.; Siemiarczuk, A.; Cowley, D. J.; Baumann, W. *Nouv. J. Chim.* **1979**, *3*, 443.
- (29) Rettig, W. *Angew. Chem., Int. Ed. Engl.* **1986**, *25*, 971.
- (30) Dobkowski, J.; Rettig, W.; Paepow, B.; Koch, K. H.; Müllen, K.; Lapouyade, R.; Grabowski, Z. R. *New J. Chem.* **1994**, *18*, 525.
- (31) Baumgarten, M.; Müller, U.; Bohnen, A.; Müllen, K. *Angew. Chem.* **1992**, *194*, 482; *Angew. Chem., Int. Ed. Engl.* **1992**, *31*, 448.
- (32) Müller, U.; Adam, M.; Müllen, K. *Chem. Ber.* **1994**, *127*, 437.
- (33) Müller, U.; Mangel, T.; Müllen, K. *Macromol. Rapid Commun.* **1994**, *15*, 45.
- (34) Baumgarten, M.; Müller, U. *Synth. Met.* **1993**, *55–57*, 4755.
- (35) Müller, U.; Baumgarten, M. *J. Am. Chem. Soc.* **1995**, *117*, 5840.
- (36) Whitton, A. J.; Kumberger, O.; Müller, G.; Schmidbaur, H. *Chem. Ber.* **1990**, *123*, 1931.
- (37) Müller, U.; Enkelmann, V.; Adam, M.; Müllen, K. *Chem. Ber.* **1993**, *126*, 1217.
- (38) Mataga, N.; Nishikawa, S.; Asahi, T.; Okada, T. *J. Phys. Chem.* **1990**, *94*, 1443.
- (39) Hirata, Y.; Okada, T.; Mataga, N.; Nomoto, T. *J. Phys. Chem.* **1992**, *96*, 6559.
- (40) Vogel, M.; Rettig, W. *Ber. Bunsen-Ges. Phys. Chem.* **1987**, *91*, 1241.
- (41) Förster, T. *Pure Appl. Chem.* **1962**, *4*, 121. *Ibid.* **1963**, *7*, 73.
- (42) Lippert, E. *Z. Elektrochem.* **1957**, *61*, 962.
- (43) Mataga, N.; Kaifu, Y.; Koizumi, M. *Bull. Chem. Soc. Jpn.* **1955**, *28*, 690.
- (44) Liptay, W. In *Excited States*; Lim, E. C., Ed.; Academic Press: New York, 1974; Vol. 1, p 129.
- (45) Rettig, W. In *Electron Transfer I*; Mattay, J., Ed.; Topics in Current Chemistry, Vol. 169; Springer Verlag: Berlin, 1994; p 253.
- (46) Klock, A. M.; Rettig, W. *Pol. J. Chem.* **1993**, *67*, 1375.
- (47) Stolarczyk, L.; Piela, L. *Chem. Phys.* **1984**, *85*, 451.
- (48) Rettig, W. *Appl. Phys.* **1988**, *45*, 145.
- (49) Birks, J. B. In *Photophysics of Aromatic Molecules*; Wiley-Interscience: London, 1970.